

# Control of cardiac alternans in a mapping model with memory

Elena Tolkacheva<sup>1</sup>, Mónica M. Romeo<sup>2</sup>, Daniel J. Gauthier<sup>1,3</sup>

<sup>1</sup>*Department of Physics*, <sup>2</sup>*Mathematics Department*,

<sup>3</sup>*Department of Biomedical Engineering*,

*and Center for Nonlinear and Complex Systems*,

*Duke University, Durham, North Carolina 27708, USA*

(Dated: October 31, 2018)

## Abstract

We investigate a map-based model of paced cardiac muscle in the presence of closed-loop feedback control. The model relates the duration of an action potential to the preceding diastolic interval as well as the preceding action potential duration and thus has some amount of ‘memory.’ We find that the domain of control depends on this memory, independently of the specific functional form of the map. The memory-dependent domain of control can encompass large feedback gains, thus providing the first possible explanation of the recent experimental results of Hall *et al.* [Phys. Rev. Lett, **88**, 198102 (2002)] on controlling alternans in small pieces of rapidly-paced cardiac muscle.

Sudden cardiac death, primarily caused by ventricular arrhythmias, is a major public health problem: it is one of the leading causes of mortality in the western world. A possible precursor of some arrhythmias is the beat-to-beat variation of the cardiac electrical excitation occurring at fast heart rates [1, 2]. This variation appears as a sequence of long-short-long-short cycles (termed alternans) in important physiological characteristics such as action potential duration (APD) and conduction time. A focus of recent theoretical and experimental studies is to investigate the mechanisms causing alternans and to terminate this response pattern using closed-loop feedback methods developed by the nonlinear dynamics community. Suppressing such alternans may then prevent the onset of fibrillation [3].

Over the last few years, several studies have demonstrated that alternans can be suppressed with dynamic feedback control of the pacing interval [4, 5, 6, 7, 8]. Control of alternans in the conduction time across the atrioventricular (AV) node has been demonstrated in both *in vitro* rabbit hearts [5] and *in vivo* human hearts [8]. The observed AV-nodal alternans are known to be well described by a one-dimensional map-based mathematical model [8]. The model can be used to predict the range of control parameters that stabilize the desired response patterns.

Recently, Hall *et al.* [4] demonstrated successful control of alternans in small pieces of *in vitro* paced bullfrog ventricles. Understanding how to control ventricular myocardium is important because it is the primary substrate for fibrillation. Controlling alternans in ventricular myocardium was expected to be more difficult than controlling AV-nodal alternans because past research suggests that its dynamics is more complicated. On the contrary, the experiments described in Ref. [4] demonstrated that alternans could be suppressed over a wide range of control parameters and over the entire range of pacing rates for which alternans was observed. The observations were compared to the predictions of two map-based mathematical models. Fitting the bifurcation diagrams of the mathematical models to the experimental data did not produce good fits for their domains of control. Specifically, control of alternans was observed for feedback gains as large as four in the experiments, whereas the models predicted that the gain must be less than  $\sim 0.4$  and limited to a small region of pacing rates near the bifurcation to alternans.

The primary purpose of this Letter is to analyze a map-based model of paced cardiac muscle in the presence of closed-loop feedback control. The model contains some degree of ‘memory’ so its dynamics displays higher-dimensional behavior. We find that the domain of

control can encompass large feedback gains, qualitatively consistent with the experiments of Hall *et al.* Our results demonstrate that higher-dimensional effects can enhance the effectiveness of control under the appropriate conditions. This may lead eventually to the development of methods for *in vivo* control of whole-heart functions. Future experiments are needed to determine whether the specific form of memory considered here is displayed by cardiac tissue. Nevertheless, our results indicate the importance of memory in the control of alternans.

To set the stage for understanding the behavior of the higher-dimensional model, we first consider a simpler one-dimensional map that contains no memory. This mapping model is given by [9, 10]

$$A_{n+1} = f(D_n), \tag{1}$$

where  $A_{n+1}$  is the APD generated by the  $(n + 1)^{st}$  stimulus, and  $D_n$  is the  $n^{th}$  diastolic interval (DI), *i.e.* the interval during which the tissue recovers to its resting state after the end of the previous ( $n^{th}$ ) action potential. We illustrate a typical bifurcation diagram in Fig. 1a. Note that the tissue has a stable 1:1 response pattern (every stimulus elicits an action potential of equal duration) for long pacing intervals (slow pacing rate). As the pacing interval decreases (faster pacing), the 1:1 response becomes unstable and a transition to alternans (2:2 response) occurs. At even faster pacing rates, the 2:2 response pattern becomes unstable and is replaced by a stable 2:1 response where an action potential is produced by every second stimulus. For the 1:1 and 2:2 responses considered herein, the pacing relation between APD and DI is  $D_n = B - A_n$ , where  $B$  is the basic pacing interval.

For this simple model, the transition from 1:1 to 2:2 behavior shown in the Fig. 1a can be understood by investigating the restitution properties of the cardiac membrane. Specifically, to predict the pacing rates at which the 1:1 response is stable, one constructs the restitution curve (RC) by plotting APD as a function  $f$  of the preceding DI, as in (1). Nolasco and Dahlen [9] proposed that the transition to alternans occurs when the slope of the RC is equal to unity. However, recent studies [4, 11, 12, 13, 14] have shown that the slope of the RC at the onset of alternans can be significantly larger than unity and thus this criterion fails to predict the existence of alternans in some cases. Later in the paper, we analyze the map (1), independently of the specific form of the function  $f$ , in the presence of closed-loop feedback control and discuss why it fails to explain the experimental observations. In contrast to the

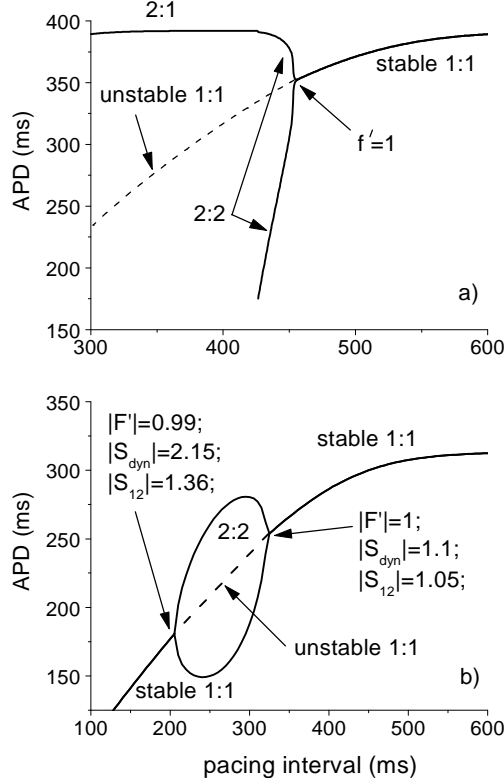


FIG. 1: Bifurcation diagrams showing existence of alternans for a) the memoryless mapping model (1) and b) the mapping model (2) with memory. Arrows indicate the points where slopes are determined. Dashed lines show unstable 1:1 response. For a),  $f(D_n) = A_1 - A_2 \exp(-D_n/\tau)$ , where  $A_1 = 392$  ms,  $A_2 = 525.3$  ms,  $\tau = 40$  ms [9]. For the mapping model (2), a specific form of the function  $F$  is taken from Refs. [14, 18], where all parameters have their typical values except  $\tau_{sopen} = 50$  ms.

memoryless model (1), we find that a cardiac mapping model of the form

$$A_{n+1} = F(A_n, D_n) \quad (2)$$

can possess a domain of control that encompasses large control gains, independently of the specific form of  $F$ . This model has some amount of memory because it relates the duration of the next action potential both to the previous DI and to the previous APD, *i.e.*, the history of the dynamical system. Several previous studies [11, 15, 16, 17] indicate that higher-dimensional behavior (so-called memory effects) is present in real cardiac tissue and thus has to be taken into account in order to correctly predict the onset of alternans. The general form of this model was first introduced by Otani and Gilmour [15] to explain

empirical observations from paced dog cardiac Purkinje fibers. More recently, a specific form of  $F$  was derived analytically [18] from a three-current ionic model [19].

Our analysis of the model (2) shows that it displays rate-dependent restitution so that there exist two primary types of RCs (the dynamic and S1-S2 RCs), which can be measured independently using different pacing protocols [14]. In the *dynamic pacing protocol*, the pacing interval  $B_1$  is held fixed until the tissue reaches equilibrium, and then progressively shortened. This yields pairs of steady-state values  $(A^*, D^*)$  for each  $B_1$ . In the *S1-S2 pacing protocol*, a premature stimulus (“S2”) is delivered at an interval  $B_2$  after pacing the tissue with a sufficiently large number of “S1” stimuli at a pacing interval  $B_1$  so that the tissue reaches equilibrium. The S1-S2 RC is determined by measuring the resulting APD for various coupling intervals  $B_2$ . Experimental studies have shown that the S1-S2 and dynamic RCs differ significantly, and have different slopes (denoted as  $S_{12}$  and  $S_{dyn}$ , respectively). This is consistent with the predictions of the mapping model (2). The transition to alternans is governed by the combination of the slopes  $S_{dyn}$  and  $S_{12}$ , so that alternans can exist when

$$|F'| = \left| 1 - \left( 1 + \frac{1}{S_{dyn}} \right) S_{12} \right| \geq 1, \quad (3)$$

where  $F'$  is the full derivative of  $F$ , with respect to  $A_n$ , evaluated at a fixed point [14]. Note that  $S_{dyn} = S_{12}$  when there is no memory in the model, and that they differ substantially when there is large memory. A typical bifurcation diagram showing alternans in the mapping model (2) is presented in Fig. 1b, where the slopes of the RCs are different and do not equal unity at the onset of alternans.

We now consider control of alternans in both models (1) and (2). To suppress alternans and stabilize the 1:1 pattern, Hall *et al.* [4] adjusted the pacing period by an amount given by

$$\varepsilon_n = -\gamma(A_{n-1} - A_{n-2}) \quad (4)$$

where  $\gamma$  is the feedback gain. Control is initiated by adjusting the basic pacing interval  $B$  by  $\varepsilon_n$ . Applying the control technique to the mapping model (1) yields

$$A_{n+1} = f(D_n) = f(B + \varepsilon_n - A_n). \quad (5)$$

The linearization of (5) in a neighborhood of the fixed point (when  $A_n = A^*$  and  $\varepsilon_n = 0$ ) is

$$A_{n+1} = A^* + \left. \frac{\partial f}{\partial A_n} \right|_{f.p.} (A_n - A^*) + \left. \frac{\partial f}{\partial \varepsilon_n} \right|_{f.p.} \varepsilon_n, \quad (6)$$

where  $f.p.$  denotes evaluation at the fixed point. Since the controlled pacing relation is  $D_n = B + \varepsilon_n - A_n$ , the derivatives in (6) are

$$\left. \frac{\partial f}{\partial A_n} \right|_{f.p.} = - \left. \frac{\partial f}{\partial \varepsilon} \right|_{f.p.} = - \left. \frac{df}{dD_n} \right|_{f.p.} \equiv \mu. \quad (7)$$

We rewrite expressions (4) and (6) in matrix form as

$$\begin{pmatrix} \delta_{n+1} \\ e_{n+1} \\ \alpha_{n+1} \end{pmatrix} = \begin{pmatrix} \mu & -\gamma\mu & 0 \\ -1 & 0 & 1 \\ 1 & 0 & 0 \end{pmatrix} \begin{pmatrix} \delta_n \\ e_n \\ \alpha_n \end{pmatrix}, \quad (8)$$

where  $\delta_n = A_n - A^*$ ,  $e_n = \varepsilon_n/\gamma$ , and  $\alpha_n = \delta_{n-1}$ . Control is successful when the eigenvalues of (8) fall within the unit circle in the complex plane. This occurs when  $\mu$  and  $\gamma$  lie within the region defined by the curves

$$\mu = 1, \quad \gamma = \frac{1 + \mu}{2\mu}, \quad \gamma = \frac{1 - \mu - \sqrt{(1 - \mu)^2 + 4}}{2\mu}, \quad (9)$$

as shown in Fig. 2a. Condition (9) defines the domain of control for the mapping model (1). Note that the domain does *not* depend on the specific functional form of  $f$ , but only on the value of its derivative  $\mu$  evaluated at the fixed point. Alternans may exist in the uncontrolled mapping model (1) when  $\mu \leq -1$ . The domain of control indicates the values of the gain  $\gamma$  that should be used to establish control of alternans for different values of the Floquet multiplier  $\mu$ , which describes the stability of the map in the absence of control. Note that the gain necessary to establish control in the region where alternans exist in the absence of control is small ( $0 < \gamma < \sqrt{2} - 1$ ), in contradiction with the experimental observations [4] where  $\gamma$  can be as large as 4. Very different behavior is found for the mapping model (2) with memory. In the presence of control, Eq. (2) becomes

$$A_{n+1} = F(A_n, D_n) = F(A_n, B + \varepsilon_n - A_n). \quad (10)$$

Linearizing (10) in a neighborhood of the fixed point, we find that

$$A_{n+1} = A^* + F' (A_n - A^*) + \left. \frac{\partial F}{\partial \varepsilon_n} \right|_{f.p.} \varepsilon_n. \quad (11)$$

where

$$F' = \left. \frac{\partial F}{\partial A_n} \right|_{f.p.} - \left. \frac{\partial F}{\partial D_n} \right|_{f.p.} \equiv \mu, \quad \left. \frac{\partial F}{\partial \varepsilon_n} \right|_{f.p.} = \left. \frac{\partial F}{\partial D_n} \right|_{f.p.} = S_{12}. \quad (12)$$

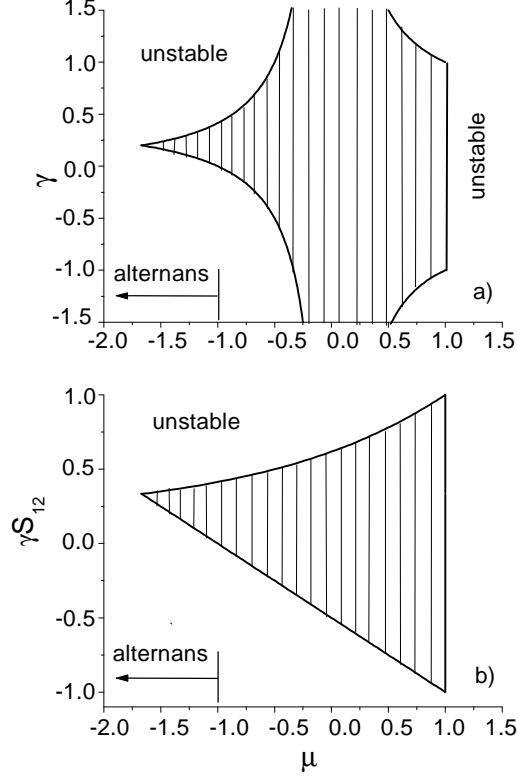


FIG. 2: Domains of control of alternans (shaded region) for a) the memoryless model (1) and b) the model with memory (2). Alternans may exist in the absence of control when  $\mu \leq -1$ .

As in Eq. (7), we denote  $\mu$  as a full derivative of  $F$ , evaluated at the fixed point. As seen from Eq. (3), the condition for the existence of alternans in the absence of control is given by  $\mu \leq -1$ . Note that the value of  $S_{12}$  does not predict the existence of alternans; instead, it characterizes the immediate response of the tissue to small perturbations from the fixed point, as was shown in Ref. [14]. Hence, we expect that  $S_{12}$  is more relevant for determining the effects of control, whereas  $\mu$  dictates the stability of the steady-state response of the tissue.

We can rewrite expressions (4) and (11) in matrix form, using the same local variables as in (8),

$$\begin{pmatrix} \delta_{n+1} \\ e_{n+1} \\ \alpha_{n+1} \end{pmatrix} = \begin{pmatrix} \mu & \gamma S_{12} & 0 \\ -1 & 0 & 1 \\ 1 & 0 & 0 \end{pmatrix} \begin{pmatrix} \delta_n \\ e_n \\ \alpha_n \end{pmatrix}. \quad (13)$$

The only difference between the matrices describing the controlled dynamics for the maps

with and without memory is the term containing the control gain  $\gamma$ . In the memoryless mapping model (1), the magnitude of perturbation sensitivity is proportional to the full derivative  $\mu$ , whereas it is proportional to the slope  $S_{12}$  of the S1-S2 RC in the mapping model with memory (2). When there is no memory,  $S_{12} = -\mu$ , whereas they can differ substantially when memory is present.

By analyzing (13), we find that control is successful when  $\mu$  and  $\gamma S_{12}$  lie within the region defined by the curves

$$\begin{aligned} \mu &= 1, & \gamma S_{12} &= -(\mu + 1)/2, \\ \gamma S_{12} &= -\left(1 - \mu - \sqrt{(1 - \mu)^2 + 4}\right) / 2. \end{aligned} \tag{14}$$

Similar to the previous model, the domain of control (14) does not depend on the specific form of the function  $F$ . We only need to know the values of the full derivative  $\mu$  and the slope of the S1-S2 RC  $S_{12}$  (evaluated at the fixed point) to determine whether it is possible to establish control. Figure 2b depicts the domain of control for the one-dimensional mapping model with memory (2) according to conditions (14). Alternans may exist in the uncontrolled system when  $\mu \leq -1$ . It can be seen from Fig. 2b that the value of  $\gamma S_{12}$  necessary to establish control for this region is relatively small ( $0 < \gamma S_{12} < \sqrt{2} - 1$ ). However, the actual control gain  $\gamma$  can be larger or smaller than this range depending on the value of  $S_{12}$ . Our predictions are consistent with our earlier expectations that  $S_{12}$  influences the effects of control since it quantifies the response of the tissue (in equilibrium) to a sudden perturbation, which the controller attempts to cancel.

Comparing our predictions to experiments is not possible at this time because no experiments have measured the slope of the S1-S2 RC *evaluated at the fixed point* [20]. Most of the experiments (see, for instance, Refs. [17, 21]) used S1-S2 pacing protocol in which the ‘‘S1’’ interval was either fixed or set to only a few different values. Instead, to make a direct comparison of the domain of control obtained using mapping model (2) to the one obtained experimentally in Ref. [4], we need to know the slope of the S1-S2 RC  $S_{12}$  at each point on the dynamic RC, *i.e.*, for different S1. The value  $S_{12}$  can be greater or less than one, depending on the specific form of  $F$  or the specific type of tissue. For example,  $S_{12} > 1$  for the function  $F$  used to generate the plot shown in Fig. 1b. Hence, the control gain  $\gamma$  must be less than  $(\sqrt{2} - 1)$  to be in the region where control is effective. However, preliminary, experiments with bullfrog cardiac muscle indicate that  $S_{12}$  can be relatively small (less than

0.4 and as small as 0.05) at the onset of alternans [22] and thus the control gain could be large.

Thus, the experimentally measured domain of control may be consistent with the predictions of the controlled map with memory (2) if  $S_{12}$  is truly less than one in bullfrog. The map without memory (1) does not agree with experiments as demonstrated by Fig. 2a and as noted previously in Ref. [4]. Our analysis is the first to suggest that memory effects may substantially enlarge the domain of control, regulated by  $S_{12}$ . Future experiments are needed to clarify the effects of memory on control.

A limitation of our analysis is that the extent of cardiac memory is only one previous beat in the model (2), so that the memory is short-term. However, some studies indicate that long-term memory effects are present in real cardiac tissue [21] that might be described using a long-term memory mapping model [12, 16]. In this model, an additional memory variable is introduced, which is assumed to accumulate during the APD and dissipate during the DI. Analysis of this model [12] confirms that the slope of the dynamic RC does not predict the transition to alternans, but it was shown in Ref. [4] that a specific form of such a memory model cannot explain the experiments on control of alternans. We believe that a generalization of the mapping model (2) that includes long-term memory as in [12, 16] may be a fruitful direction for future investigations.

We gratefully acknowledge the support of the National Science Foundation under Grant PHY-9982860 and DMS-9983320 (M.M.R).

- 
- [1] A. Karma, *Chaos* **4**, 461 (1994).
  - [2] R.F. Gilmour, Jr., D.R. Chialvo, *J. Cardiovasc. Electrophysiol.* **10**, 1087 (1999).
  - [3] B. Echebarria, and A. Karma, *Chaos* **12**, 533 (2002).
  - [4] G.M. Hall, and D.J. Gauthier, *Phys. Rev. Lett.* **88**, 198102 (2002).
  - [5] K. Hall, D.J. Christini, M. Tremblay, J.J. Collins, L. Glass, and J. Billette, *Phys. Rev. Lett.* **78**, 4518 (1997).
  - [6] W.-J. Rappel, F. Fenton and A. Karma, *Phys. Rev. Lett.* **83**, 456 (1999).
  - [7] D.J. Gauthier, and J.E.S. Socolar, *Phys. Rev. Lett.* **79**, 4938 (1997).
  - [8] D.J. Christini, K.M. Stein, S.M. Markowitz, S. Mittal, D.J. Slotwiner, M.A.Scheiner, S. Iwai,

- and B.B. Lerman, Proc. Nat. Acad. Sci. **98**, 5827 (2001).
- [9] J.B. Nolasco, and R.W. Dahlen, J. Appl. Physiol. **25**, 191 (1968).
- [10] M. Guevara, G. Ward, A. Shrier, and L. Glass, Computers in Cardiology (IEEE Computer Society, Silver Spring, MD, 1984), p.167.
- [11] G.M. Hall, S. Bahar, and D.J. Gauthier, Phys. Rev. Lett. **82**, 2995 (1999).
- [12] J.J. Fox, E. Bodenschatz, and R.F. Gilmour, Phys. Rev. Lett. **89**, 138101 (2002).
- [13] I. Banville, and R.A. Gray, J Cardiovasc. Electrophysiol. **13**, 1141 (2002).
- [14] E.G. Tolkacheva, D.G. Schaeffer, D.J. Gauthier, and W. Krassowska, Phys. Rev. E. **67**, 031904 (2003).
- [15] N.F. Otani, and R.F. Gilmour, Jr., J. Theor. Biol. **187**, 409 (1997).
- [16] D.R. Chialvo, D.C. Michaels, and J. Jalife, Circ. Res. **66**, 525 (1990).
- [17] R.F. Gilmour, Jr., N.F. Otani, and M.A. Watanabe, Am. J. Physiol. **272**, H1826 (1997).
- [18] E.G. Tolkacheva, D.G. Schaeffer, D.J. Gauthier, and C.C. Mitchell, Chaos **12**, 1034 (2002).
- [19] F. Fenton, and A. Karma, Chaos **8**, 20 (1998).
- [20] We note that a pacing protocol has been suggested in [18] for easily determining  $S_{dyn}$ ,  $S_{12}$ , and  $F'$  (evaluated at the fixed points) in experiments.
- [21] M.A. Watanabe, and M.L. Koller, Am. J. Physiol. **282**, H1534 (2002).
- [22] S. Sau and H. Dobrowolny, private communication.